Research Article
Open Access
CrossMark

LEKTI, a physiological inhibitor of multiple serine proteinases, blocks migration and invasion of head and neck squamous cell carcinoma (HNSCC) cells

Abstract

Serine Protease Inhibitor Kazal-type 5 (SPINK5) gene encodes 3 different Lympho-Epithelial Kazal-Type-Inhibitor (LEKTI) isoforms which are organized into longer than 15, 15, and 13 inhibitory domains. We identified LEKTI by its constitutive expression in normal oral mucosa and lost or down regulated expression in matched tumor specimens of patients with head and neck squamous cell carcinoma (HNSCC). Previously, we showed that recombinant full-length LEKTI and rLEKTI fragments inhibit the activity of plasmin, subtilisin A, cathepsin G, neutrophil elastase, trypsin, caspase 14, and kallikreins (KLK) 5, 6, 7, 13, and 14 to varied extents. Here, we show that LEKTI protein is absent in HNSCC OSC19, Tu138, Tu177, and UMSCC1 lines. We then determined the consequences of LEKTI re-expression on migration and invasion, adhesion and gene expression profile of HNSCCOSC19 and UMSCC1 lines. We demonstrate that LEKTI expressing OSC19 and UMSCC1 clones show markedly reduced migration and invasion. Moreover, LEKTI expressing OSC19 clones show striking morphological changes and enhanced adhesionon type I, III, IV, and V collagens, fibronectin, and laminin5.In addition, we show that exogenous r-LEKTI blocks migration of OSC19-parental cells in a dose and time dependent manner. Microarray analysis identified 186 genes which are differentially regulated in both OSC19 LEKTI clones.mMP-14, KLK5, and ADAM8 are down regulated whilemMP-3, LEKTI, DSC2 and DSC3are up-regulated in OSC19 LEKTI clones. RT-PCR and Western blot results confirmed microarray results formMP-14 andmMP-3in OSC19 LEKTI clones. In addition we discover thatmMP-9 protein expression and pro-MMP-9 activity are severely reduced in LEKTI expressing clones as shown by WB and zymogram. Together, this work provides mechanistic insights into how loss of LEKTI protein expression promotes an invasive phenotype in HNSCC tumors.

Keywords: SPINK5, LEKTI, invasion, migration, adhesion, mMPs, HNSCC, KLK

Volume 1 Issue 3 - 2014

Arumugam Jayakumar,[1,2] Chandrani Chattopadhyay,[1] Hua-Kang Wu,[1] Katrina Briggs,[1] Ying Henderson,[1] Yaan Kang,[1] Latha Ramdas,[3] Shikha Sharma,[1] Venugopal Radjendirane,[2] Thomas D Shellenberger,[1] Gary L Clayman[1]

[1]Department of Head and Neck Surgery, University of Texas MD Anderson Cancer Center, USA
[2]Department of Experimental Therapeutics, University of Texas MD Anderson Cancer Center, USA
[3]Department of Experimental Radiation Oncology, University of Texas MD Anderson Cancer Center, USA

Correspondence: Arumugam Jayakumar, Department of Head and Neck Surgery, University of Texas MD Anderson Cancer Center, Houston, Texas 77030, USA, Email ajayakum@mdanderson.org

Received: July 01, 2014 | **Published:** July 08, 2014

Abbreviations: LEKTI, lympho-epithelial kazal-type-inhibitor; SPINK5, serine protease inhibitor kazal-type 5; KLK, kallikreins; kDa, kilodaltons; RT-PCR, reverse-transcriptase polymerase chain reaction; SD, standard deviation of the mean

Introduction

Lympho-epithelial kazal-type-inhibitor (LEKTI)1 was named by one of the original groups who cloned this protein's gene to reflect the observed pattern of its expression in both epithelial tissue and leukocytes.[1] It was later identified as the same gene as the defective gene in Netherton's syndrome, SPINK5 (serine protease inhibitor Kazal-type 5).[2] Netherton's syndrome is a genetic disorder characterized by congenital ichthyosis, hair shaft abnormalities, immune deficiency, elevated immunoglobulin E (IgE) concentration, and failure to thrive.[2–13] SPINK5 encodes the LEKTI protein which consists of 1064 amino acids organized into 15 potential inhibitory domains on the basis of the furin cleavage sites found within the full-length molecule. At the N-terminus is a secretory signal peptide sequence consisting of 22 amino acids.[14] Two of the 15 LEKTI domains (domains 2 and 15) resemble typical Kazal-type serine proteinase inhibitors; the remaining 13 domains share partial homology to Kazal-type inhibitors but lack one of the three conserved Kazal-type disulfide bridges.[15]

We and others identified SPINK5 as one of the genes down regulated in head and neck squamous cell carcinoma (HNSCC).[16,17] We cloned the cDNA encoding the 125-kDa isoform and established that recombinant pro-LEKTI is a potent inhibitor of multiple serine proteinases implicated in metastasis and angiogenesis. Moreover, rLEKTI did not inhibit the cysteine proteinase papain or cathepsin K, L, or S. We further showed that recombinant pro-LEKTI was very efficiently cleaved *in vitro* by furin into five major and thirteen minor proteolytic fragments.[18] In the course of studies aimed at understanding the structure and function of some of these domains, we demonstrated that recombinant LEKTI6-9′ inhibited trypsin and subtilisin A but not plasmin, cathepsin G, or elastase.[19] We also produced a battery of LEKTI monoclonal antibodies and demonstrated that several of these LEKTI antibodies including 1C11G6 reacted specifically with pro-LEKTI, LEKTI domains 1-6, 6-9, 9-12, and 12-15.[20] We demonstrated that the N-terminal signal peptide is required for LEKTI import into the ER and ordered the cleavage products on the 125kDa pro-LEKTI from the amino- to carboxy-terminal as follows: 37-, 40-, and 60kDa.[21] In our subsequent work, we characterized the interaction of two recombinant LEKTI domains 6-8 and 9-12 with recombinant rhK5 and recombinant rhK7.[22] We showed that both fragments inhibited rhK5 similarly and established that LEKTI, at least in fragment form, is a potent inhibitor of rhK5 and that this protease may be a target of

LEKTI in human skin. In our later studies we discovered that KLK5, KLK6, KLK13 and KLK14 were potently inhibited by rLEKTI (1-6), rLEKTI (6-9') and rLEKTI (9-12).[23,24] We also assessed the basis for phenotypic variations in patients with "mild", "moderate" and "severe" NS.[25] We observed that the magnitude of KLK activation correlated with both the barrier defect and clinical severity, and inversely with residual LEKTI expression and LEKTI co-localizes within the stratum corneum (SC) with kallikreins 5 and 7 and inhibits both KLKs. Recently, we demonstrated that caspase 14 is inhibited by full-length LEKTI and 5 recombinant fragments of LEKTI to varied extents.[26]

In the present study, we stably re-expressed LEKTI in HNSCC cells and evaluated the effects of LEKTI re-expression on cellular proliferation, morphology, adhesion, invasion and expression of key mMPs involved in tumor progression. LEKTI re-expression in OSC19 cells causes striking morphological changes, strongly enhances adhesion, markedly decreased migration and invasion. Stable re-expression of LEKTI in OSC19 cells resulted in markedly decreased levels of mMP-9 and mMP-14. Furthermore, these results demonstrate a novel negative regulatory role for LEKTI in modulating the production of keymMPs involved in ECM degradation and suggest that loss of LEKTI in HNSCC tumor cells could have a pivotal role in HNSCC progression.

Materials and methods

Materials

The following reagents were obtained commercially as indicated: Human embryonic kidney cells (HEK 293T) (American Type Culture Collection, Manassas, VA); primary normal epidermal keratinocytes (HNEKs) and keratinocyte growth medium (Cambrex Biosciences, Walkersville, MD); OSC-19 from Dr. There OPTIMEM (Life Technologies, Rockville, MD); precast sodium dodecyl sulfate (SDS)-polyacrylamide gels, prestained markers, gelatin Zymogram gels (Bio-Rad Laboratories, Hercules, CA); nitrocellulose membrane (Schleicher & Schull BioScience, Keene, NH); YM3 Centriplus (Millipore, Bedford, MA); anti-LEKTI mAb1C11G6 (Zymed Laboratories, San Francisco, CA); collagens, I, III, and V, fibronectin, laminin-5, BSA, GAPDH, anti-β actin, anti-MMP-9, and anti-MMP–14 antibodies (Sigma-Aldrich, St. Louis, MO), horseradish peroxidase-conjugated goat-anti-mouse IgG (H+L) (Jackson ImmunoResearch Laboratories, West Grove, PA); lipofectamine 2000 and pcDNA3.1 (-) (Invitrogen, Carlsbad, CA); ECL kit (Amersham Bioscience Corporation, Piscataway, NJ); Kodak X-AR5 films (Eastman Kodak, Rochester, NY); restriction endonucleases and polymerase chain reaction reagents (New England Biolabs, Beverely, MA); BD BioCoat Tumor Invasion System (BD Biosciences); r-LEKTI is purified in our laboratory as described previously.[18]

Cell culture and transfections

The HNSCC cell lines (Tu 138 and JMAR) were established at The University of Texas M. D. Anderson Cancer Center. Dr. Tom Carey at the University of Michigan developed UMSCC1. A human oral squamous cell carcinoma cell strain, OSC19, was obtained from Dr. Theresa Whiteside and maintained in Dulbecco's modified Eagle's medium (DMEM) supplemented with 10% fetal bovine serum, 2mM glutamine, and antibiotics. HEK 293T were cultured in DMEM supplemented with 10% FBS and 2mM glutamine. HNEKs were cultured in keratinocyte growth medium containing low-calcium. All cells were cultured at 37°C in humidified incubator with 5% CO_2 and 95% air. All cells were cultured at 37°C in humidified incubator with 5% CO_2 and 95% air.

To clone the pro-LEKTI expression plasmid, 3.24Kb BamHI-KpnI fragment from LEKTI/pFASTBAC1, clone #4 was sub cloned into pcDNA 3.1. The pro-LEKTI expression plasmid encodes the entire full-length LEKTI polypeptide and has a hexahistidine tag at its C-terminus. 293T cells transfected with this construct expressed LEKTI. At 24h and 48h post transfection, LEKTI is detected within the cells and in the medium. In the medium LEKTI processed LEKTI fragments are also detected with LEKTI mAb 1C11G6. In order to delete the signal sequence, this clone is digested with NotI and EcoRI and ligated to a PCR fragment lacking this signal sequence. The pro-LEKTI-Δ1-22 expression plasmid encodes the full-length LEKTI polypeptide without the N-terminus secretory signal sequence and has a hexahistidine tag at its C-terminus. When transfected into 293T cells, very little intracellular protein is observed. Following the verification of these expression clones, HNSCC cells were transfected with these constructs and stable clones were selected after G418 (0.5mg/ml) selection. We also performed transient transfection of OSC-19 and HEK 293T cells with these constructs. Cells were plated in 60×15-mm tissue culture dishes grown to 70% confluence, and transiently transfected with 2.0μg each of pro-LEKTI expression plasmid DNA or pro-LEKTI-Δ1-22 expression plasmid DNA or control vector plasmid DNA using Lipofectamine 2000 according to the manufacturer's instructions. Approximately 50% transfection efficiency was achieved as determined by transfection with a GFP control plasmid.

LEKTI secretion assays

Cells were washed twice in phosphate buffered saline (PBS) and resuspended in 4ml serum-free media for 24 hrs. The conditioned media was ten-fold concentrated by centrifugation using Millipore-YM3 Centriplus units (3,000 MWCO) and assayed for protein concentrations.[27] To examine LEKTI expression in protein lysates, the adherent cells were trypsinized and solubilized in 100μl of ice-cold radio immunoprecipitation assay (RIPA) buffer containing 1% Nonidet P-40, 1.0% deoxycholate, 0.1% SDS, 50mM Tris-HCl, (pH 7.5), 150mM NaCl, 2mM EDTA and a mixture of protease inhibitors.

Western blot

Proteins or concentrated culture supernatants were mixed with 2×gel loading buffer (4% SDS; 20% glycerol; 120mM Tris-HCl, pH 6.8; 0.01% bromophenol blue; with or without 10 % β-mercaptoethanol), heated to 95°C for 5min, and resolved by SDS-PAGE (10% gel). Electrophoretic transfer of proteins from the polyacrylamide gel onto a nitrocellulose membrane (Schleicher & Schull BioScience, Inc., Keene, NH) was achieved by using amini-trans blot electrophoretic cell (Bio-Rad) at 25V for 16h at 4°C. After blocking the nitrocellulose membrane overnight at room temperature with 3% BSA, it was incubated for 2h at room temperature with primary and 1h with the secondary antibody. The immunoblot was visualized using the chemiluminescence-ECL substrate and exposed to X-ray Hyperfilm MP for 1-3min.

Adhesion assays

The 96-well high binding non- tissue culture plates were coated with equimolar amounts of type I, III, IV, and V collagens, fibronectin, and laminin-5, and vitronectin (100nM) for 3-4 hours at 37°C. Control wells received BSA alone. Wells were blocked with 5% BSA for 45minutes prior to use. HNSCC cells are added at 2X104 cells/

well in serum-free DMEM. Cells were allowed to adhere at 37°C for 90minutes. Following washing, remaining adherent cells were fixed with 0.5% crystal violet in methanol/water. Background binding was assessed using coated wells but received no cells and subtracted from experimental values. The crystal violet incorporated into cell were collected in 1% SDS and quantified by measuring A_{590}.

Migration and Invasion assays

Cell migration and invasion was determined using BD BioCoat Tumor Invasion System that consists of a 24-Mutliwell-insert plate in which a PET membrane (8µm pore size) has been coated without or with Matrigel. OSC19-parent, OSC19-Vector-1, OSC19-LEKTI-11, and OSC19-LEKTI-17 clones suspended in medium without serum were added to the upper wells of inserts, which were then were placed into lower wells containing NIH 3T3 supernatant containing 10% fetal calf serum as a chemo attractant and allowed to invade for 24h in a CO_2 humidified incubator. To measure migration alone, parallel wells were set up with control inserts that lacked a Matrigel coating. Alternatively, OSC19-parent cells suspended in medium without serum and treated with recombinant pro-LEKTI were added to the upper wells of control inserts which were then were placed into lower wells containing NIH 3T3 supernatant containing 10% fetal calf serum as a chemo attractant and allowed to migrate for 24h in a CO_2 humidified incubator. At the end of each assay, the lower sides of inserts containing migrated or invaded cells are stained and photographed.

Gelatin zymography

OSC19-parent, OSC19-Vector-1, OSC19-LEKTI-11, and OSC19-LEKTI-17 clones grown in DMEM media containing 10% fetal calf serum and 2mM glutamine were washed twice in phosphate buffered saline (PBS) and resuspended in 4ml of serum-free media for 24hrs. Thereafter, 1ml of supernatants was collected, centrifuged (300xg) for 10min to remove non-adherent cells and thereafter, supernatants were centrifuged a second time (5000xg) for 10min to remove cell debris and nuclei. Supernatants were concentrated (10X) by centrifugation using Millipore-YM3 Centriplus units (3,000 MWCO). 5µl concentrated supernatants are mixed with Zymogram sample buffer in the absence of reducing agents and electrophoresed through 12% polyacrylamidegels containing 0.1% (w/v). Electrophoresis was carried out at 125 V. After electrophoresis, the gel was washed twice with 100ml of 2.5% (v/v) Triton X-100 at 22°C for 30min to remove SDS, and three times for 10min with H_2O to remove Triton X-100. The gel was incubated in 50mM Tris-HCl, 0.2 M NaCl, 20mM $CaCl_2$, pH 7.4 at 37 C for 12h, stained over night with Coomassie Brilliant Blue R-250 0.5% (w/v) in 45% (v/v) methanol-10% (v/v) acetic acid and destained in the same solution without dye. The location of gelatinolytic activity is visualized as a clear band on the uniformly stained background.

Northern blot and Real time PCR

Total RNA isolation, Northern blot and Real-time PCR were performed as described earlier.[28] Total RNA was prepared using TriZol reagent (Invitrogen) according to the manufacturer's instructions. For Northern blot, 20µg total RNA was applied to a 1% formaldehyde agarose gel. After transferring RNA to Hybond-Nþ membrane (Amersham), the membrane and the filter were hybridized with ^{32}P-r-human LEKTI or ^{32}P-GAPDH. For Real-time PCR, 2µg total RNA were reverse transcribed (RT) by Superscript II (Life Technologies) in a 25µl total reaction volume containing RT buffer, random hexamers, dNTP, and RNase inhibitor (Roche Applied Science, Indianapolis, IN). Real-time PCR was performed in a 25µl total reaction volume containing 1µ of 1:10 diluted cDNA obtained from RT reaction, 12.5µl of TaqMan Universal PCR Master Mix without AmpErase UNG, and 1.25µl of specific primers for each gene on ABI Prism 7900HT (kindly provided by Dr. Adel El-Naggar from the Department of Pathology, M. D. Anderson Cancer Center). As a control, 18S primers were used, and cDNA was diluted to 1:500. Serial dilutions of the standard templates were also used for parallel amplifications. The threshold cycles (Ct) were calculated with ABI Prism 7900HT SDS software (Applied Biosystems). The quantities of samples were determined from the standard curves. Levels ofmMP-3, mMP-9 andmMP-19 mRNA were normalized to those of 18S in each sample. For statistical analysis, the Tukey HSD analysis of variance post hoc test was used as a univariate test for significant differences between the ratio means and the P value was determined. A P value of 0.05 or less was considered significant.

Microarray analysis

Total cellular RNA isolation, cDNA preparation, and microarray analysis were performed as described previously.[28,29] Briefly, hybridization to microarrays was performed using human oligonucleotide–spotted glass array with 18,861 60-mer oligos and controls produced in the Wiegand Radiation Oncology Microarray Core Facility at our institution. Hybridization was carried out for 16h at 50°C. Scanned images were quantified in Array Vision (Imaging Research, Inc., St. Catherine's, Ontario, Canada). Measurements were recorded for spot intensity, local background intensity, and signal-to-noise ratio. Spot intensity was computed as the integrated absorbance or volume in a fixed-size circle. Background intensity was computed as the median pixel value in four diamond-shaped regions at the corners of each spot. The signal-to-noise ratio was computed by dividing the background-corrected intensity by the SD of the background pixels. Quantified array data were imported into S-Plus software (Insightful Corp., Seattle, WA) for analysis. Background-corrected intensities were globally rescaled to set the 75th percentile in each channel equal to 1,024. Rescaled intensities of <128 were replaced by the threshold value; this threshold was chosen to lie just below the smallest intensity of any spot with a signal-to-noise ratio >1. Next, intensities were transformed by computing the base 2 logarithm. Finally, the log-transformed spot intensities were normalized using robust local regression. A spot was identified as differentially expressed if the mean intensity in the two channels exceeded 512 and the estimated change exceeded 2.5-fold or if the mean intensity in the two channels exceeded 256 and the estimated change exceeded 4.5-fold. The normalized data was logarithm transformed to base 2 and the mean data of the replicates was determined. The log ratio values were calculated for the clones 11 and 17 and corresponding paired vector controls. Differentially regulated mRNA between the 2 samples was identified using a paired t test. We included the complete microarray dataset as a supplementary Microsoft Excel file and also in the process of depositing our dataset to Array Express database soon.

Results and discussion

Analysis of LEKTI mRNA and LEKTI protein expression in HNSCC tumor lines

Using Northern blotting, we analyzed the expression of LEKTI mRNA in HNEK, HEK 293T-vector transfect ant, HEK 293T-LEKTI transfect ant, and HNSCC OSC19, Tu138 and Tu177 tumor lines. Northern blot analysis showed that a 3.75-kb mRNA band was detected

in HNEK and 293T cells transiently transfected with pro-LEKTI expression plasmid. This transcript is not detectable in 293T-vector transfectant and OSC19 cells but present in reduced levels in Tu177 and Tu138 cell lines. The results were consistent with the patterns of LEKTI mRNA expression previously reported for normal oral epithelium and several HNSCC cell lines including Tu138 and Tu 177 (Figure 1A).[16] Using Western blotting, we analyzed the expression of native LEKTI protein by using anti-LEKTI mAb 1C11G6 and protein lysates from HNEK, HEK 293T-vector transfectant, and HNSCC OSC19, Tu138, Tu177, and UMSCC1 tumor lines. Anti-LEKTI antibody 1C11G6 recognized a major protein of ~125kDa and amine or protein of 110kDa in HNEKs indicating robust expression of LEKTI protein; in contrast both bands were absent in all four HNSCC tumor lines (Figure 1B). The endogenously expressed 125kDa LEKTI found in HNEKs was identical to r-pro-LEKTI expressed and purified from insect cells.[18] Protein lysates from HEK 293T cell transfected with control vector showed no endogenous LEKTI expression. This Western blot signal was completely absent when a preserum was used. The results were consistent with the patterns of LEKTI protein expression reported for normal kidney and colon tissues.[30]

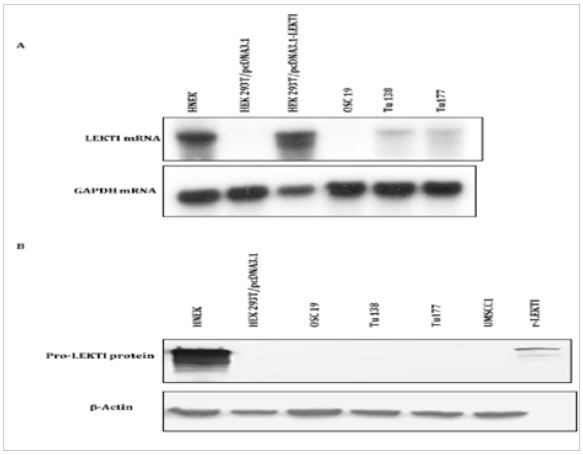

Figure 1 LEKTI is absent from the established HNSCC lines. A: LEKTI mRNA in HNEK, 293T-vector transfectant, 293T-LEKTI tranfectant, and HNSCC tumor lines. Northern blot analysis showed that a 3.75-kb mRNA band was detected in HNEK and 293T-LEKTI transfectant. This transcript is not detectable in 293T-vectortransfectant and OSC19cells but present in reduced levels in Tu177 and Tu138 cell lines. B: LEKTI protein expression in HNEK, 293T-vector transfectant, and HNSCC tumor lines. Western blot analysis with the anti-LEKTI mAb1C11G6 showed the 125 kDa native pro-LEKTI protein in 50µg cell lysates of HNEK cells. This band is not detectable in 293T-vector transfectant, OSC19, Tu177, Tu138, and UMSCC1 cell lines. r-LEKTI detection serves as a positive control. Actin detection allows the comparison between samples loading. Results are representative of three independent experiments using cultures from three different transfections.

Stable LEKTI re-expression inhibits matrigel migration and invasion of OSC19

To understand the impact of LEKTI re-expression in HNSCC cells, we cloned a native LEKTI cDNA fragment encoding pro-LEKTI protein into the expression vector pcDNA3.1, transfected into OSC19 and UMSCC1 cells and isolated several stable clones after G418 (0.5mg/ml) selection for almost a month. We selected one OSC19-vector clone 1; two OSC19-LEKTI clones 11 and 17 and one UMSCC1 clone 2 for further studies. We examined the cell lysates and conditioned medium from these clones for the expression of recombinant and for the presence of processed LEKTI fragments by Western blot assays (Figure 2A). Stable expression of recombinant LEKTI in these three clones is processed and secreted into the medium similar to what we reported for HNEK cells.[21] We recently showed that native pro-LEKTI in HNEK cells is processed and secreted into the medium by an ER/Golgi-dependent pathway. Furthermore, we demonstrated that endogenous furin plays a pivotal role in the processing pro-LEKTI. Now, we show that stably expressed recombinant LEKTI in OSC19 and UMSCC1cells is also similarly processed and secreted into the medium.

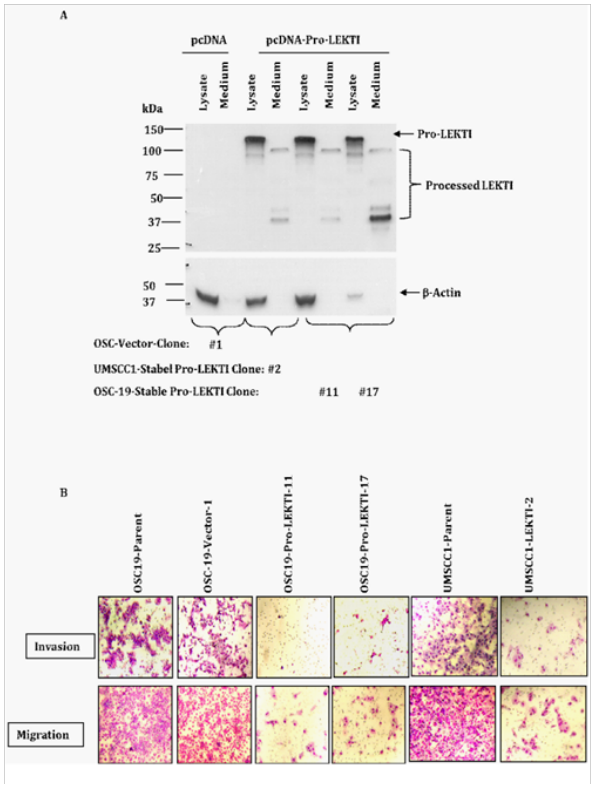

Figure 2 Stable LEKTI re-expression inhibits matrigel migration and invasion of OSC19 and UMSCC1. A: LEKTI protein in cell lysate and medium of OSC19-Vector clone 1, OSC19-LEKTI clones 11 and 17 and UMSCC-LEKTI clone 2. Western blot analysisshowed the 125 kDa native pro-LEKTI protein in cell lysates and about 37-, 40-, and 60 (very faint) kDa processed LEKTI fragments in the medium of OSC19-LEKTI clones 11 and 17 and UMSCC-LEKTI clone 2 (The 100 kDa band represents intermediate cleavage product of LEKTI). These bands are not detectable in OSC19-Vector clone 1. Actin detection allows the comparison between samples loading. B: Stable LEKTI expression results in inhibition of migration and invasion of HNSCC tumor lines OSC19 and UMSCC1 *in vitro*.

In our pilot studies we noticed no migration of any of our HNSCC lines in conditions in which no chemo attractant was added. Hence, we compared the chemotactic migration of various HNSCC tumor lines in response to 5% FCS or NIH3T3 supernatant in an uncoated control insert plate with a PET membrane containing 8micron pores. We found that NIH 3T3 supernatant proved a more optimal chemo attractant with a 30% increase in cell migration compared to 5% FBS. In addition, we observed a 2- to 3.5-fold increase in the migration of OSC19 compared with UMSCC1. On the basis of these results, we used the NIH 3T3 supernatant as a chemo attractant in our subsequent assays. In each of two LEKTI expressing clones of OSC-19, invasion was dramatically reduced compared to parental and vector cells (Figure 2B). Likewise, in LEKTI expressing clones of UMSCC2 invasion were significantly reduced compared to parental cells. We found more number of OSC19 parental and vector cells and

UMSCC1 parental cells stained under migration than under invasion assays. Surprisingly, in each of two LEKTI expressing clones of OSC19 and one LEKTI expressing clones of UMSCC1, migration also was dramatically reduced compared to parental and vector cells. On the basis of these results, we conclude that LEKTI in tumor cells most likely functions in the extracellular tumor microenvironment and furthermore the levels of LEKTI in LEKTI transfected HNSCC cell model are comparable with those existing naturally. These data suggest that stable LEKTI expression results in inhibition of migration and invasion of HNSCC tumor lines *in vitro*.

Transient LEKTI re-expression inhibits matrigel migration of OSC19

To determine the effect of LEKTI re-expression on cellular migration, we transiently transfected OSC19 cells with pro-LEKTI or pro-LEKTI deleted for the N-terminal secretory sequence. Using these transfectants we first characterized LEKTI expression and then performed migration assays. We observed that the expression of carboxy-terminal hexa-histidine tagged pro-LEKTI with it signal sequence and its processed LEKTI fragments was abundant in the cell lysates and supernatant as shown by its immuno reactivity with LEKTI mAb (Figure 3A). In contrast, deletion of the signal peptide resulted in markedly low levels of pro-LEKTI-Δ1-22 in the soluble fraction of cell lysates (Figure 3A), and we could not detect any processed LEKTI fragments in the conditioned medium (Figure 3A). These results are in agreement with our previous studies where we demonstrated that pro-LEKTI is processed and secreted into the medium in HEK 293T cells transiently transfected with the pro-LEKTI expression plasmid whereas the level of pro-LEKTI-Δ1-22 in lysates and medium went down dramatically.[21]

The migration of OSC19 cells transfected with empty vector was comparable to their un-transfected OSC19 parental cells (Figure 3B). In contrast, the migration of OSC19 Pro-LEKTI transfectent through Matrigel was inhibited by more than 95% (P=0.001). On the other hand, the migration of pro-LEKTI-Δ1-22 transfectant through Matrigel was not affected and it is comparable to OSC19 cells transfected with empty vector and un-transfected OSC19 parental cells. On the basis of these results we conclude that LEKTI protein is directly responsible for the inhibition of OSC19 migration and also functional LEKTI is required to exert its inhibitory effect on migration.

Exogenous r-LEKTI inhibits matrigel invasion and migration of OSC19

Next, we tested if exogenous r-LEKTI can elicit the inhibition of migration of OSC parental cells. Recombinant pro-LEKTI was expressed and purified from insect cells as described previously.[18,23,31] OSC19 parental cells are treated without r-LEKTI or with 10nM, 30nM, and 100nM r-LEKTI for 24h or with 30nM r-LEKTI for 0h, 6h, 18h, and 24h and then cells were allowed to migrate for 24h with control inserts that lacked a Matrigel coating in a CO_2 humidified incubator. Migration assays show that r-LEKTI inhibits the migration of OSC19 cells in a dose and time dependent fashion (Figure 4). No inhibition of migration was observed after 6 h incubation with 30nM r-LEKTI but 18h incubation resulted in substantial inhibition and 24h incubation showed almost a total inhibition.

LEKTI re-expression enhances adhesion and regulates the morphology of OSC19

We observed that both OSC19 LEKTI clones required more time for trypsinization when passaging the cells. To test this observation and determine the adhesion of cells to extracellular matrix constituents in relation to LEKTI expression, we performed assays of OSC19 cell adhesion to collagen type I, collagen type III, collagen type IV, collagen type V, laminin-5, fibronectin, and vitronectin. After 3h of adhesion, each of two LEKTI-expressing clones demonstrated increased adhesion to collagen I, III, IV, IV, laminin-5, and fibronectin compared to parental and vector cells (Figure 5A). The increase in adhesion of OSC19-LEKTI clones to collagen I, III, IV, IV, laminin-5, and fibronectin was 1300, 100, 150, 200, 300 and 40% respectively. In contrast, when plated on vitronectin, both control and LEKTI stable clones showed a similar extent of adhesion. Additionally, the morphology of LEKTI-expressing OSC19 clones was drastically altered from the parental and vector cells. After 4days of culture in normal tissue culture plates, the parental and vector cells formed thin and spreading stellate shapes with numerous processes (Figure 5B). In contrast, each of two LEKTI-expressing clones of OSC19 formed polygonal shapes and aggregated into compacts clumps. On the basis of these results, we conclude that re-expressed LEKTI in HNSCC cells lead to a cell type specific increase in adhesion onto specific extracellular matrix substrates. These observations suggest that LEKTI expression regulates cell morphology to result in a more differentiated phenotype resembling the architecture of squamous epithelium.

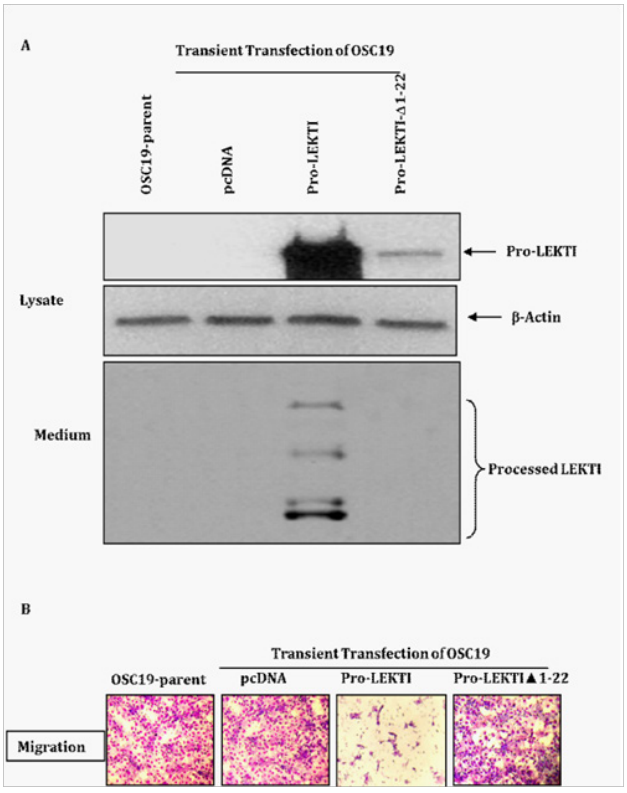

Figure 3 Transient LEKTI re-expression inhibits matrigel migration of OSC19. A: LEKTI protein expression in OSC19 cells transiently transfected with vector DNA or pro-LEKTI or pro-LEKTI-Δ1-22expression plasmid DNA. Western blot analysis showed the 125 kDa native pro-LEKTI protein in lysates and about 37-, 40-, and 60kDa processed LEKTI fragments in the medium of OSC19 (the 100 kDa band represents intermediate cleavage product of LEKTI). These bands are not detectable in OSC19-Vector transfectant and a very faint band is visible in OSC19-pro-LEKTI-Δ1-22expression plasmid DNA. Actin detection allows the comparison between samples loading. B: Migration of OSC19 cells transiently transfected with vector DNA or pro-LEKTI or pro-LEKTI-Δ1-22expression plasmid DNA. The migration of OSC19 cells transfected with empty vector was comparable to their parental line OSC19. The migration of OSC19 pro-LEKTI but not OSC19-pro-LEKTI-Δ1-22through Matrigel was inhibited by more than 90% (P = 0.001). Results are representative of three independent experiments using cultures from three different transfections.

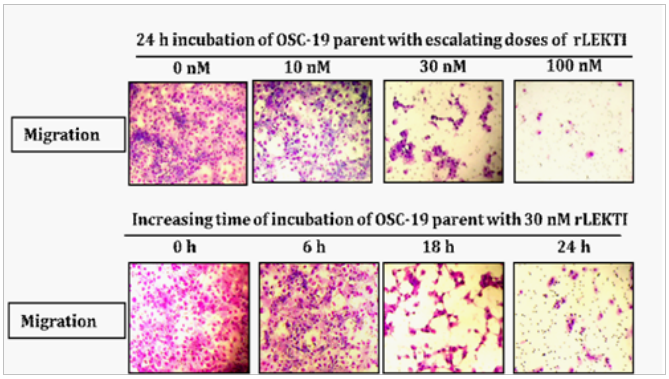

Figure 4 Exogenous r-LEKTI inhibits matrigel invasion and migration of OSC19. Migration of OSC-Parent. OSC19 parent cells are treated without r-LEKTI or with 10nM, 30nM, and 100nM r-LEKTI for 24h or with 30nM r-LEKTI for 0h, 6h, 18h, and 24h and then cells were allowed to invade for 24h with control inserts that lacked a Matrigel coating in a CO_2 humidified incubator. Migration assays show that r-LEKTI inhibits the migration of OSC19 cells in a dose and time dependent fashion. Results are representative of three independent experiments using r-LEKTI from three different purifications.

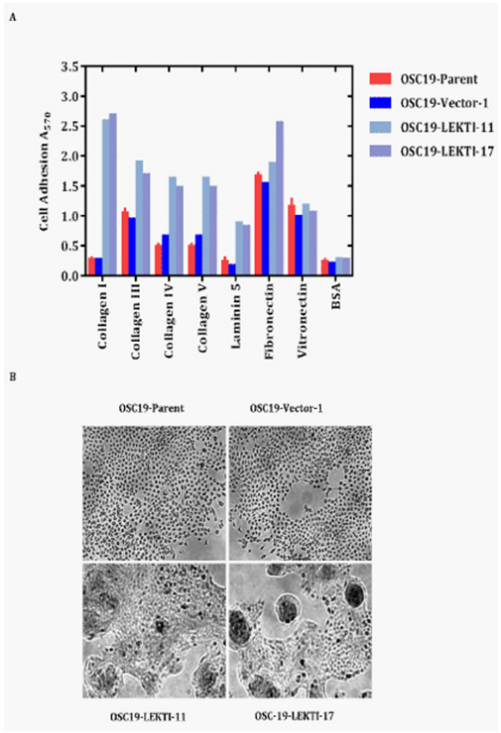

Figure 5 LEKTI re-expression enhances adhesion and regulates the morphology of OSC19. A: Adhesion of OSC-Parent, OSC19-Vector clone 1, OSC19-LEKTI clones 11 and 17 on type I, III, IV, and V collagens, laminin-5, fibronectin, vitronectin, and BSA. Each of the two LEKTI-expressing clones demonstrated significantly increased adhesion ($P< 0.005$)to collagen I, III, IV,V, and laminin-5, compared to parental and vector cells. The percentage increase in adhesion of OSC19-LEKTI cells to collagen I, III, IV,V, and laminin-5, was 1300, 100, 150, 150, and 300 %, respectively. In contrast, when plated on vitronectin, fibronectin, or BSA, both control and LEKTI stable clones showed a similar extent of adhesion. B: Photographs of OSC-Parent, OSC-Vector-1, and OSC-19-LEKTI clones 11 and 17. After 4 days of culture in normal tissue culture plates, the parental and vector cells formed thin and spreading stellate shapes with numerous processes. In contrast, each of two LEKTI-expressing clones of OSC19 formed polygonal shapes and aggregated into compacts clumps. Results are representative of two independent experiments using cultures from two different platings.

LEKTI re-expression negatively regulates expression ofmMP-9 and -14

Microarray analysis identified 186 genes which are differentially regulated between LEKTI clones in comparison with the vector transfected OSC19. Among them,mMP-14,mMP-8, KLK5, and ADAM8 are down regulated andmMP-3, LEKTI, DSC2 and DSC3 are up-regulated in LEKTI clones (Table 1) of the four classes of proteolytic enzymes, which include mMPs, serine proteinases, cysteine proteinases, and aspartate proteinases, them MPs are most important to the process of metastasis.[32,33] To examine the expression of mMPs in relation to LEKTI expression we performed analysis of mMPs in OSC19 parental, vector, and LEKTI- expressing clones 11 and 17. By real-time PCR, each LEKTI-expressing clone showed a decrease in mMP-14 and an increase inmMP-3 transcript (Figure 6A). These results confirmed our microarray results on these two mMPs (Table 2). In addition, we found out that each LEKTI-expressing clone showed a decrease inmMP-9 mRNA expression relative to parental and vector cells (Figure 6A). Consistent with down regulation ofmMP-9 and mMP-14 mRNA expression, each LEKTI-expressing clone showed dramatic reduction in mMP-9 and –14-protein level relative to parental and vector cells (Figure 6B). We confirmed this finding by zymogram showing a decrease in mMP-9 protein activity levels in response to LEKTI expression (Figure 6B).

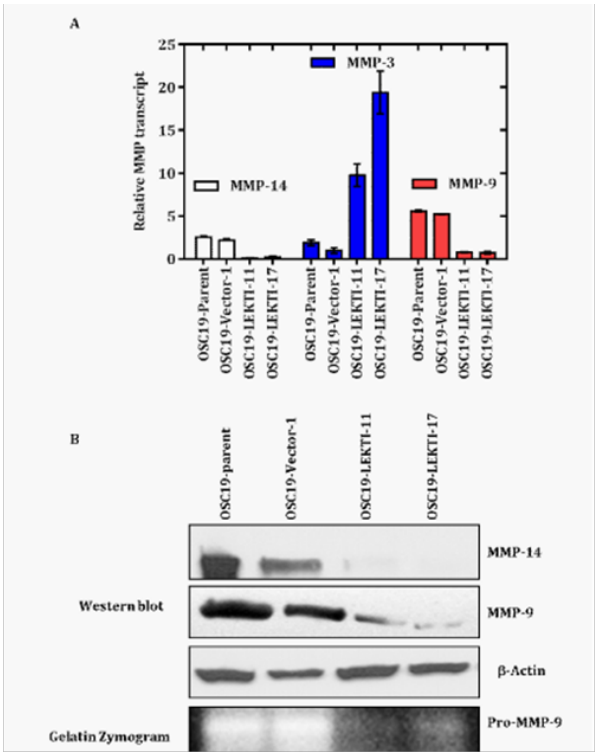

Figure 6 LEKTI re-expression negatively regulates expression of MMP-9 and -14. A: Relative level of MMP-14, MMP-9 and MMP-3 transcriptin OSC-Parent, OSC19-Vector clone 1, OSC19-LEKTI clones 11 and 17 as determined by RT-PCR. MMP-14 and MMP-9 transcripts went down while MMP-3 transcript went up in both clones. B: MMP-9 and MMP-14 protein expression in OSC-Parent, OSC19-Vector clone 1, OSC19-LEKTI clones 11 and 17. Western blot analysis with the anti- MMP-9 and anti-MMP-14 showed the MMP-9 and MMP-14 proteins in 50µg cell lysates of OSC-Parent and OSC19-Vector clone 1. These bands are present markedly reduced levels in OSC19-LEKTI clones 11 and 17. Actin detection allows the comparison between samples loading. Gelatin zymogram shows pro-MMP-9 activity in OSC-Parent and OSC19-Vector clone 1 and markedly reduced pro-MMP-9 activity in OSC19-LEKTI clones 11 and 17. Results are representative of three independent experiments using cultures from three different platings.

Citation: Jayakumar A, Chattopadhyay C, Wu HK, et al. LEKTI, a physiological inhibitor of multiple serine proteinases, blocks migration and invasion of head and neck squamous cell carcinoma (HNSCC) cells. *MOJ Proteomics Bioinform.* 2014;1(3):57–71. DOI: 10.15406/mojpb.2014.01.00015

Table 1 L4_S0335 and L4_S0337: Common genes that are differentially regulated between Clone 11 and Clone17 in comparison with the vector transfected OSC-19. The positive logratio values are for genes that are upregulated in the clones and the negative logratio values are genes downregulated in the clones

Spot Location	UGRepAcc	Symbol	Name	Clone 11_log ratio	Clone 17_log ratio	Up regulation		Down regulation	
						Foldchange_ clone11	Foldchange_ clone17	Foldchange_ clone11	Foldchange_ clone17
C-6:23-8	NM_001512	GSTA4	glutathione S-transferase A4	15.86	14.37	59575.04	21128.97		
A-8:12-11	NM_002373	MAP1A	microtubule-associated protein 1A	15.86	14.99	59300.62	32530.79		
B-3:17-5	NM_006536	CLCA2	chloride channel, calcium activated, family member 2	14.95	2.02	31659.09	4.04		
D-7:16-2	AL050367	LOC221061	hypothetical protein LOC221061	14.30	14.73	20215.06	27092.83		
B-2:6-14	NM_018372	RIF1	receptor-interacting factor 1	14.15	4.94	18239.04	30.70		
A-8:4-3	XM_290809	TAF4B	TAF4b RNA polymerase II, TATA box binding protein (TBP)-associated factor, 105kDa	13.92	15.21	15523.79	37944.50		
B-6:1-23	NM_006180	NTRK2	neurotrophic tyrosine kinase, receptor, type 2	13.87	4.72	14952.63	26.31		
A-5:16-1	NM_025247	ALDH2	aldehyde dehydrogenase 2 family (mitochondrial)	13.45	3.30	11189.55	9.84		
A-6:20-14	NM_001449	FHL1	four and a half LIM domains 1	13.34	14.21	10337.80	18959.51		
C-7:24-1	NM_000691	ALDH3A1	aldehyde dehydrogenase 3 family, memberA1	9.53	6.70	737.55	103.98		
D-2:12-5	NM_002421	MMP1	matrix metalloproteinase 1 (interstitial collagenase)	8.14	14.06	281.19	17059.21		
A-1:2-10	NM_002638	PI3	protease inhibitor 3, skin-derived (SKALP)	7.84	3.57	229.76	11.84		
B-2:13-12	NM_002964	S100A8	S100 calcium binding protein A8 (calgranulin A)	6.32	5.85	79.70	57.61		
D-3:7-14	NM_004561	OVOL1	ovo-like 1(Drosophila)	6.10	3.79	68.59	13.83		
C-4:25-15	NM_006783	GJB6	gap junction protein, beta 6 (connexin 30)	6.07	14.86	67.11	29790.05		
A-8:24-15	NM_014220	TM4SF1	transmembrane 4 superfamily member 1	5.53	5.90	46.05	59.70		
D-5:17-6	NM_006227	PLTP	phospholipid transfer protein	5.38	5.30	41.55	39.44		
C-2:4-11	NM_002272	KRT4	keratin 4	5.37	2.57	41.47	5.92		
B-2:11-1	NM_005329	HAS3	hyaluronan synthase 3	5.34	4.21	40.39	18.45		
A-3:25-9	NM_153490	KRT13	keratin 13	5.32	3.73	40.06	13.27		
B-1:15-1	NM_022746	FLJ22390	hypothetical protein FLJ22390	5.29	2.64	39.20	6.24		
D-3:8-6	NM_001353	AKR1C1	aldo-keto reductase family 1, member C1 (dihydrodiol dehydrogenase 1; 20-alpha (3-alpha)-hydroxysteroid dehydrogenase)	5.26	6.41	38.19	85.32		
B-1:23-10	NM_003914	CCNA1	cyclin A1	5.23	5.48	37.61	44.58		
C-7:1-3	NM_005986	SOX1	SRY (sex determining region Y)-box 1	5.20	5.19	36.72	36.40		

Citation: Jayakumar A, Chattopadhyay C, Wu HK, et al. LEKTI, a physiological inhibitor of multiple serine proteinases, blocks migration and invasion of head and neck squamous cell carcinoma (HNSCC) cells. *MOJ Proteomics Bioinform.* 2014;1(3):57–71. DOI: 10.15406/mojpb.2014.01.00015

TableContinued....

Spot Location	UGRepAcc	Symbol	Name	Clone 11_log ratio	Clone 17_log ratio	Up regulation		Down regulation	
						Foldchange_ clone11	Foldchange_ clone17	Foldchange_ clone11	Foldchange_ clone17
D-5:15-6				5.18	6.15	36.18	70.99		
B-3:19-5	NM_002422	MMP3	matrix metalloproteinase 3 (stromelysin 1, progelatinase)	5.04	5.65	33.01	50.37		
D-5:18-3	NM_181353	ID1	inhibitor of DNA binding 1, dominant negative helix-loop-helix protein	4.90	4.26	29.80	19.13		
B-2:19-14	NM_003125	SPRR1B	small proline-rich protein 1B (cornifin)	4.61	2.79	24.46	6.94		
C-1:18-14	NM_017459	MFAP2	microfibrillar-associated protein 2	4.57	13.81	23.77	14373.79		
D-3:18-8	NM_007366	PLA2R1	phospholipase A2 receptor 1, 180kDa	4.51	4.30	22.74	19.64		
D-6:21-8	NM_000584	IL8	interleukin 8	4.42	2.03	21.34	4.08		
A-6:12-11	NM_001978	EPB49	erythrocyte membrane protein band 4.9 (dematin)	4.21	3.03	18.56	8.16		
C-7:13-8	NM_024829	FLJ22662	hypothetical protein FLJ22662	4.10	2.68	17.20	6.40		
C-3:1-7	NM_145791	MGST1	microsomal glutathione S-transferase 1	4.06	5.85	16.67	57.66		
D-7:5-9	NM_014656	KIAA0040	KIAA0040 gene product	3.92	2.46	15.12	5.51		
B-6:14-2	NM_001964	EGR1	early growth response 1	3.88	4.25	14.75	19.01		
D-7:13-24	NM_144665	SESN3	sestrin 3	3.85	5.80	14.41	55.80		
C-6:14-23	AK001903		CDNA FLJ11041 fis, clone PLACE1004405	3.77	4.94	13.67	30.61		
B-1:15-6	NM_002130	HMGCS1	3-hydroxy-3-methylglutaryl-Coenzyme A synthase 1 (soluble)	3.75	2.73	13.48	6.62		
C-4:22-8	NM_006846	SPINK5	serine protease inhibitor, Kazal type, 5	3.73	14.85	13.31	29489.80		
C-1:22-9	NM_002275	KRT15	keratin 15	3.57	2.40	11.88	5.28		
D-7:20-3	NM_004473	FOXE1	forkhead box E1 (thyroid transcription factor 2)	3.54	3.21	11.66	9.22		
D-3:2-18	NM_032508	FAM11A	family with sequence similarity 11, member A	3.39	4.87	10.47	29.26		
C-4:17-23	AK026158	LOC348938	hypothetical protein LOC348938	3.37	4.67	10.37	25.42		
B-5:5-1	NM_007286	SYNPO	synaptopodin	3.37	3.52	10.37	11.46		
B-7:13-13	NM_000299	PKP1	plakophilin 1 (ectodermal dysplasia/skin fragility syndrome)	3.36	2.90	10.24	7.48		
C-5:3-4	NM_001452	FOXF2	forkhead box F2	3.35	2.70	10.22	6.50		
D-7:16-23	NM_031455	CCDC3	coiled-coil domain containing 3	3.33	3.36	10.03	10.26		
D-8:25-5	NM_012244	SLC7A8	solute carrier family 7 (cationic amino acid transporter, y+ system), member 8	3.23	5.26	9.36	38.32		
B-2:24-8	NM_002996	CX3CL1	chemokine (C-X3-C motif) ligand 1	3.22	6.33	9.29	80.62		

TableContinued....

Spot Location	UGRepAcc	Symbol	Name	Clone 11_log ratio	Clone 17_log ratio	Up regulation		Down regulation	
						Foldchange_ clone11	Foldchange_ clone17	Foldchange_ clone11	Foldchange_ clone17
B-6:6-19	NM_004988	MAGEA1	melanoma antigen, family A, 1 (directs expression of antigen MZ2-E)	3.13	4.28	8.74	19.45		
D-7:24-15	NM_018950	HLA-F	major histocompatibility complex, class I, F	3.10	2.71	8.60	6.52		
D-2:13-16	AF001893		MRNA; cDNA DKFZp686L01105 (from clone DKFZp686L01105)	3.08	2.59	8.43	6.04		
A-7:8-7	NM_194298	SLC16A9	solute carrier family 16 (monocarboxylic acid transporters), member 9	3.07	3.48	8.41	11.18		
B-3:22-3	NM_016307	PRRX2	paired related homeobox 2	3.05	2.72	8.26	6.57		
D-5:11-12	NM_001775	CD38	CD38 antigen (p45)	3.04	2.37	8.25	5.16		
C-8:25-6	NM_001360	DHCR7	7-dehydrocholesterol reductase	3.00	2.53	8.01	5.80		
D-5:24-12	NM_005130	HBP17	heparin-binding growth factor binding protein	3.00	2.25	8.00	4.77		
C-2:11-23	BX640887		CDNA clone IMAGE:3880075, partial cds	2.98	3.23	7.88	9.40		
D-1:7-6	NM_001823	CKB	creatine kinase, brain	2.95	4.54	7.73	23.24		
D-4:21-6	NM_002083	GPX2	glutathione peroxidase 2 (gastrointestinal)	2.88	3.50	7.38	11.31		
B-6:15-10	NM_006763	BTG2	BTG family, member 2	2.82	2.25	7.05	4.77		
B-5:14-12	NM_003028	SHB	SHB (Src homology 2 domain containing) adaptor protein B	2.80	16.66	6.97	103825.37		
B-5:17-11	NM_004949	DSC2	desmocollin 2	2.78	2.04	6.86	4.12		
B-5:19-11	NM_002214	ITGB8	integrin, beta 8	2.73	3.22	6.65	9.32		
C-7:19-9	NM_000422	KRT17	keratin 17	2.73	2.91	6.61	7.51		
A-5:13-16	NM_000692	ALDH1B1	aldehyde dehydrogenase 1 family, member B1	2.61	2.33	6.12	5.03		
D-2:12-17	NM_032333	MGC4248	hypothetical protein MGC4248	2.59	2.35	6.04	5.09		
A-1:15-11	NM_005901	MADH2	MAD, mothers against decapentaplegic homolog 2 (Drosophila)	2.59	4.06	6.02	16.71		
D-8:16-14	NM_000852	GSTP1	glutathione S-transferase pi	2.58	2.27	5.98	4.82		
C-4:23-20	AK000090		CDNA FLJ20083 fis, clone COL03440	2.55	2.84	5.85	7.14		
C-4:24-20	AK000794		CDNA FLJ20787 fis, clone COL02178	2.46	3.16	5.51	8.95		
C-3:18-14	NM_003480	MAGP2	Microfibril-associated glycoprotein-2	2.43	6.55	5.37	93.83		
D-3:22-7	NM_006822	RAB40B	RAB40B, member RAS oncogene family	2.39	2.64	5.25	6.22		
B-5:16-8				2.38	4.25	5.21	19.02		
A-8:16-9	NM_006096	NDRG1	N-myc downstream regulated gene 1	2.31	2.61	4.95	6.10		

TableContinued....

Spot Location	UGRepAcc	Symbol	Name	Clone 11_log ratio	Clone 17_log ratio	Up regulation		Down regulation	
						Foldchange_ clone11	Foldchange_ clone17	Foldchange_ clone11	Foldchange_ clone17
C-1:12-10	NM_004431	EPHA2	EphA2	2.27	2.30	4.83	4.94		
D-6:8-3	NM_018555	ZNF331	zinc finger protein 331	2.27	3.64	4.81	12.44		
B-7:19-6	NM_014427	CPNE7	copine VII	2.26	2.79	4.80	6.90		
C-2:8-7	XM_370652	DNCH2	dynein, cytoplasmic, heavy polypeptide 2	2.26	2.04	4.79	4.11		
A-1:25-13	NM_002820	PTHLH	parathyroid hormone-like hormone	2.26	3.14	4.78	8.82		
C-4:18-11	NM_018103	LRRC5	leucine rich repeat containing 5	2.23	3.37	4.70	10.32		
A-8:13-1				2.21	2.60	4.62	6.07		
D-7:21-1	NM_000104	CYP1B1	cytochrome P450, family 1, subfamily B, polypeptide 1	2.21	2.32	4.61	5.00		
A-1:20-17	NM_052932	PORIMIN	pro-oncosis receptor inducing membrane injury gene	2.18	2.04	4.53	4.12		
C-2:1-3	NM_138281	DLX4	distal-less homeobox 4	2.17	3.85	4.50	14.41		
D-4:19-17	AK024449	PP2135	PP2135 protein	2.16	3.26	4.48	9.61		
D-1:15-13	NM_001657	AREG	amphiregulin (schwannoma-derived growth factor)	2.16	2.43	4.47	5.37		
D-1:13-2	NM_005642	TAF7	TAF7 RNA polymerase II, TATA box binding protein (TBP)-associated factor, 55kDa	2.16	2.30	4.46	4.92		
B-3:19-12	NM_000597	IGFBP2	insulin-like growth factor binding protein 2, 36kDa	2.16	2.24	4.45	4.72		
C-1:1-18	BQ431041		LOC388279 (LOC388279), mRNA	2.15	2.72	4.44	6.60		
B-2:17-21	NM_007006	CPSF5	cleavage and polyadenylation specific factor 5, 25 kDa	2.14	2.36	4.41	5.13		
B-4:11-17	NM_006096	NDRG1	N-myc downstream regulated gene 1	2.14	2.39	4.41	5.24		
D-6:15-7				2.09	2.05	4.24	4.15		
A-1:17-3	NM_016265	ZNF325	zinc finger protein 325	2.08	2.29	4.24	4.89		
B-4:16-11	NM_024423	DSC3	desmocollin 3	2.08	2.43	4.23	5.39		
C-4:17-7	NM_006598	SLC12A7	solute carrier family 12 (potassium/chloride transporters), member 7	2.03	2.62	4.08	6.13		
D-5:8-6	NM_031220	PITPNM3	PITPNM family member 3	2.01	2.94	4.02	7.70		
A-7:1-16	NM_015714	G0S2	putative lymphocyte G0/G1 switch gene	-2.02	-2.59	0.25	0.17	4.067469826	6.02797569
D-4:7-17	NM_000202	IDS	iduronate 2-sulfatase (Hunter syndrome)	-2.03	-2.75	0.25	0.15	4.077710921	6.75034936
D-3:6-9	NM_000202	IDS	iduronate 2-sulfatase (Hunter syndrome)	-2.04	-2.87	0.24	0.14	4.101875487	7.29841054
C-5:25-16	NM_138768	MYEOV	myeloma overexpressed gene (in a subset of t(11;14) positive multiple myelomas)	-2.05	-2.49	0.24	0.18	4.144497434	5.62253016

TableContinued....

Spot Location	UGRepAcc	Symbol	Name	Clone 11_log ratio	Clone 17_log ratio	Up regulation		Down regulation	
						Foldchange_ clone11	Foldchange_ clone17	Foldchange_ clone11	Foldchange_ clone17
D-3:23-9	NM_018222	PARVA	parvin, alpha	-2.05	-2.56	0.24	0.17	4.145801706	5.88473227
B-7:4-23	NM_182507	LOC144501	hypothetical protein LOC144501	-2.07	-4.11	0.24	0.06	4.208758818	17.3227835
C-8:22-13	NM_020799	AMSH-LP	associated molecule with the SH3 domain of STAM (AMSH) like protein	-2.08	-2.34	0.24	0.20	4.214203909	5.04987403
A-5:10-10	NM_003087	SNCG	synuclein, gamma (breast cancer-specific protein 1)	-2.11	-2.18	0.23	0.22	4.30472467	4.53020489
D-7:12-1	NM_014297	ETHE1	ethylmalonic encephalopathy 1	-2.14	-2.15	0.23	0.23	4.419559792	4.43492191
A-2:18-8	NM_002543	OLR1	oxidised low density lipoprotein (lectin-like) receptor 1	-2.18	-4.00	0.22	0.06	4.518721967	15.9888148
D-3:16-8	NM_000963	PTGS2	prostaglandin-endoperoxide synthase 2 (prostaglandin G/H synthase and cyclooxygenase)	-2.18	-2.20	0.22	0.22	4.533257978	4.60992803
C-8:1-10	NM_022481	ARAP3	ARF-GAP, RHO-GAP, ankyrin repeat and plekstrin homology domains-containing protein 3	-2.18	-2.59	0.22	0.17	4.542590739	6.02919293
C-7:5-7	NM_023927	NS3TP2	HCV NS3-transactivated protein 2	-2.19	-3.26	0.22	0.10	4.566722537	9.58576143
D-5:12-13	NM_000024	ADRB2	adrenergic, beta-2-, receptor, surface	-2.22	-2.05	0.21	0.24	4.674568202	4.13068734
D-4:19-2	NM_031283	TCF7L1	transcription factor 7-like 1 (T-cell specific, HMG-box)	-2.25	-3.09	0.21	0.12	4.77061901	8.52709149
B-7:5-9	NM_000916	OXTR	oxytocin receptor	-2.29	-2.33	0.20	0.20	4.890803849	5.0310331
A-7:6-15	NM_003289	TPM2	tropomyosin 2 (beta)	-2.32	-2.76	0.20	0.15	5.008541393	6.78462145
B-2:12-7	NM_015994	ATP6V1D	ATPase, H+ transporting, lysosomal 34kDa,V1 subunit D	-2.33	-2.16	0.20	0.22	5.025197605	4.46298352
D-3:18-11	NM_000610	CD44	CD44 antigen (homing function and Indian blood group system)	-2.34	-2.76	0.20	0.15	5.056402704	6.77232189
C-3:12-5	NM_014256	B3GNT3	UDP-GlcNAc:betaGal beta-1,3-N-acetylglucosaminyltransferase 3	-2.35	-2.53	0.20	0.17	5.084537435	5.7804644
A-5:3-14	NM_005096	ZNF261	zinc finger protein 261	-2.39	-2.39	0.19	0.19	5.248917876	5.25675946
B-4:10-12				-2.41	-2.29	0.19	0.20	5.306823008	4.88133901
A-5:16-14	NM_000224	KRT18	keratin 18	-2.43	-2.36	0.19	0.19	5.404795682	5.14281952
B-7:8-16	NM_005780	LHFP	lipoma HMGIC fusion partner	-2.47	-2.68	0.18	0.16	5.538633731	6.4003583
C-3:5-6	NM_080927	ESDN	endothelial and smooth muscle cell-derived neuropilin-like protein	-2.47	-2.22	0.18	0.21	5.549855877	4.65363937
B-6:14-9	NM_000224	KRT18	keratin 18	-2.49	-3.07	0.18	0.12	5.620597234	8.37846833

Citation: Jayakumar A, Chattopadhyay C, Wu HK, et al. LEKTI, a physiological inhibitor of multiple serine proteinases, blocks migration and invasion of head and neck squamous cell carcinoma (HNSCC) cells. *MOJ Proteomics Bioinform.* 2014;1(3):57–71. DOI: 10.15406/mojpb.2014.01.00015

TableContinued....

Spot Location	UGRepAcc	Symbol	Name	Clone 11_log ratio	Clone 17_log ratio	Up regulation		Down regulation	
						Foldchange_ clone11	Foldchange_ clone17	Foldchange_ clone11	Foldchange_ clone17
D-8:5-3	XM_172341	FLJ35036	hypothetical protein FLJ35036	-2.50	-2.40	0.18	0.19	5.643607678	5.27784987
B-4:3-8	NM_007246	KLHL2	kelch-like 2, Mayven (Drosophila)	-2.51	-2.64	0.18	0.16	5.696310881	6.23936453
C-5:6-16	NM_024074	MGC3169	hypothetical protein MGC3169	-2.52	-3.02	0.17	0.12	5.742923627	8.13173279
A-3:2-10	NM_004486	GOLGA2	golgi autoantigen, golgin subfamily a, 2	-2.53	-2.38	0.17	0.19	5.772987061	5.19065094
B-1:7-16				-2.59	-2.05	0.17	0.24	6.032982476	4.13563384
B-5:12-17	NM_005170	ASCL2	achaete-scute complex-like 2 (Drosophila)	-2.62	-2.84	0.16	0.14	6.16397665	7.15336668
A-3:7-7	NM_024527	ABHD8	abhydrolase domain containing 8	-2.62	-2.27	0.16	0.21	6.168460111	4.81227412
A-1:12-11	NM_012317	LDOC1	leucine zipper, down-regulated in cancer 1	-2.66	-2.49	0.16	0.18	6.307614839	5.60637904
D-3:1-10	NM_016445	PLEK2	pleckstrin 2	-2.68	-2.58	0.16	0.17	6.400691717	5.96001472
B-3:17-8	NM_001102	ACTN1	actinin, alpha 1	-2.68	-2.50	0.16	0.18	6.419911166	5.64413645
D-8:14-6	NM_021727	FADS3	fatty acid desaturase 3	-2.69	-2.35	0.15	0.20	6.469132441	5.0921694
C-7:8-12	NM_001430	EPAS1	endothelial PAS domain protein 1	-2.70	-3.13	0.15	0.11	6.486214515	8.72684951
A-6:12-24	NM_080927	ESDN	endothelial and smooth muscle cell-derived neuropilin-like protein	-2.74	-2.50	0.15	0.18	6.691795939	5.67460969
A-4:23-22				-2.78	-2.18	0.15	0.22	6.868454225	4.545701
A-7:1-12	NM_003246	THBS1	thrombospondin 1	-2.79	-2.44	0.14	0.18	6.907748398	5.4118483
D-3:20-21	NM_012153	EHF	ets homologous factor	-2.83	-5.45	0.14	0.02	7.127245138	43.7963006
D-7:15-10	NM_012153	EHF	ets homologous factor	-2.84	-4.87	0.14	0.03	7.16989817	29.1565438
B-6:10-12	NM_031892	SH3KBP1	SH3-domain kinase binding protein 1	-2.86	-2.36	0.14	0.20	7.241210789	5.12084435
A-8:9-24	NM_018306	FLJ11036	hypothetical protein FLJ11036	-2.87	-2.49	0.14	0.18	7.305619394	5.63444971
C-8:2-5	NM_002318	LOXL2	lysyl oxidase-like 2	-2.88	-4.15	0.14	0.06	7.337897944	17.7454702
C-7:5-1	NM_003958	RNF8	ring finger protein (C3HC4 type) 8	-2.88	-2.33	0.14	0.20	7.368691284	5.01284359
D-4:18-14	NM_003738	PTCH2	patched homolog 2 (Drosophila)	-2.91	-2.56	0.13	0.17	7.495722738	5.911008
B-3:1-13	NM_004447	EPS8	epidermal growth factor receptor pathway substrate 8	-2.96	-3.50	0.13	0.09	7.770902194	11.2762852
B-5:10-11	NM_022073	EGLN3	egl nine homolog 3 (C. elegans)	-2.96	-3.54	0.13	0.09	7.804044613	11.6098577
A-2:2-17	NM_138444	KCTD12	potassium channel tetramerisation domain containing 12	-2.97	-2.14	0.13	0.23	7.851667546	4.39601931
B-3:13-6	NM_007283	MGLL	monoglyceride lipase	-3.03	-4.63	0.12	0.04	8.146860637	24.806172
D-5:25-5	NM_005101	G1P2	interferon, alpha-inducible protein (clone IFI-15K)	-3.06	-3.45	0.12	0.09	8.326883604	10.9634954
B-2:13-10	NM_005429	VEGFC	vascular endothelial growth factor C	-3.07	-2.51	0.12	0.18	8.408091946	5.7120402
A-7:17-11	NM_005723	TM4SF9	transmembrane 4 superfamily member 9	-3.09	-2.48	0.12	0.18	8.52649501	5.5823862

TableContinued....

Spot Location	UGRepAcc	Symbol	Name	Clone 11_log ratio	Clone 17_log ratio	Up regulation		Down regulation	
						Foldchange_ clone11	Foldchange_ clone17	Foldchange_ clone11	Foldchange_ clone17
A-4:12-17	NM_153611	MGC20446	hypothetical protein MGC20446	-3.09	-3.06	0.12	0.12	8.539562097	8.34144982
A-8:7-11	NM_018192	MLAT4	myxoid liposarcoma associated protein 4	-3.17	-3.31	0.11	0.10	8.979387807	9.94098854
A-5:14-13	NM_057159	EDG2	endothelial differentiation, lysophosphatidic acid G-protein-coupled receptor, 2	-3.18	-3.02	0.11	0.12	9.055761789	8.11254773
D-8:14-5	NM_004995	MMP14	matrix metalloproteinase 14 (membrane-inserted)	-3.19	-2.47	0.11	0.18	9.124402264	5.54910849
A-3:24-10	NM_001553	IGFBP7	insulin-like growth factor binding protein 7	-3.20	-2.47	0.11	0.18	9.194347608	5.52503874
A-5:6-16	NM_003803	MYOM1	myomesin 1 (skelemin) 185kDa	-3.29	-3.91	0.10	0.07	9.774320104	15.0783315
C-2:5-5	NM_016233	PADI3	peptidyl arginine deiminase, type III	-3.30	-4.77	0.10	0.04	9.862444313	27.3226366
A-8:24-7	NM_006517	SLC16A2	solute carrier family 16 (monocarboxylic acid transporters), member 2 (putative transporter)	-3.37	-3.57	0.10	0.08	10.34882831	11.8464534
C-6:15-6	NM_012105	BACE2	beta-site APP-cleaving enzyme 2	-3.38	-2.18	0.10	0.22	10.43754205	4.54496723
A-6:13-6	NM_005672	PSCA	prostate stem cell antigen	-3.39	-3.50	0.10	0.09	10.47451419	11.2751577
A-3:8-16	NM_002273	KRT8	keratin 8	-3.45	-3.79	0.09	0.07	10.95760551	13.8757902
C-8:4-16	NM_007085	FSTL1	follistatin-like 1	-3.47	-6.65	0.09	0.01	11.11533316	100.251904
C-6:17-7	NM_004207	SLC16A3	solute carrier family 16 (monocarboxylic acid transporters), member 3	-3.51	-3.98	0.09	0.06	11.36560673	15.793495
C-4:6-11	NM_007203	PALM2	paralemmin 2	-3.51	-2.13	0.09	0.23	11.4246333	4.36597548
D-5:19-4				-3.57	-2.78	0.08	0.15	11.85742483	6.8516617
A-3:15-9	NM_000295	SERPINA1	serine (or cysteine) proteinase inhibitor, clade A (alpha-1 antiproteinase, antitrypsin), member 1	-3.61	-6.57	0.08	0.01	12.20991141	95.0583386
A-1:1-15	NM_003118	SPARC	secreted protein, acidic, cysteine-rich (osteonectin)	-3.61	-3.10	0.08	0.12	12.24073208	8.57801881
A-4:15-9				-3.65	-2.44	0.08	0.18	12.56172657	5.44344481
A-3:4-14	NM_001654	TIMP1	tissue inhibitor of metalloproteinase 1 (erythroid potentiating activity, collagenase inhibitor)	-3.71	-3.05	0.08	0.12	13.12721004	8.26900241
A-4:20-1				-3.95	-2.89	0.06	0.14	15.49965719	7.39869191
D-7:8-6	NM_021005	NR2F2	nuclear receptor subfamily 2, group F, member 2	-3.98	-3.54	0.06	0.09	15.74627136	11.6231813
B-4:12-5	NM_001109	ADAM8	a disintegrin and metalloproteinase domain 8	-4.26	-4.02	0.05	0.06	19.10086542	16.2296299
D-8:17-11	NM_001792	CDH2	cadherin 2, type 1, N-cadherin (neuronal)	-4.36	-2.91	0.05	0.13	20.529152	7.52090111
A-6:2-10	NM_182909	DOC1	downregulated in ovarian cancer 1	-4.39	-2.59	0.05	0.17	20.95746529	6.00852077

Citation: Jayakumar A, Chattopadhyay C, Wu HK, et al. LEKTI, a physiological inhibitor of multiple serine proteinases, blocks migration and invasion of head and neck squamous cell carcinoma (HNSCC) cells. *MOJ Proteomics Bioinform.* 2014;1(3):57–71. DOI: 10.15406/mojpb.2014.01.00015

TableContinued....

Spot Location	UGRepAcc	Symbol	Name	Clone 11_log ratio	Clone 17_log ratio	Up regulation		Down regulation	
						Foldchange_ clone11	Foldchange_ clone17	Foldchange_ clone11	Foldchange_ clone17
B-7:24-6	NM_024519	FLJ13725	hypothetical protein FLJ13725	-4.46	-3.29	0.05	0.10	21.95627756	9.77013135
D-2:10-11	NM_005727	TSPAN-1	tetraspan 1	-4.47	-6.29	0.05	0.01	22.16640231	78.1239771
D-5:8-10				-4.72	-4.91	0.04	0.03	26.31474624	29.984916
C-7:6-9	NM_000331	SAA1	serum amyloid A1	-5.15	-2.41	0.03	0.19	35.45660337	5.32381919
D-4:14-14	NM_012427	KLK5	kallikrein 5	-5.30	-6.55	0.03	0.01	39.43541733	93.616596
B-8:21-11	AF200348	D2S448	Melanoma associated gene	-6.08	-5.15	0.01	0.03	67.5205415	35.4459189
D-2:7-14	NM_001323	CST6	cystatin E/M	-6.35	-6.34	0.01	0.01	81.42425084	81.0151155

Table 2 Common genes that are differentially regulated between OSC19-LEKTI clone 11 in comparison with the OSC19-Vector clone 1. The negative fold change values are for genes that are down regulated and the positive fold change values are genes that are up regulated in the clone

Gene name	Fold change
MMP-14	-9.2
MMP-8	-19.5
KLK5	-93.6
ADAM8	-16.5
MMP3	+14.9
LEKTI	+80.8
DSC2	+10.8
DSC3	+5.8

Using LEKTI mAb 1C11G6, we observed that in specimens of histologically normal mucosa, LEKTI-positive staining was present in the cytoplasm of epithelial cells extending above the basal layers. Conversely, in specimens of dysplastic mucosa, LEKTI-positive staining was diminished in all layers of the epithelium. Moreover, in the majority of specimens of invasive carcinoma staining was limited to a few cells scattered within the tumor of nests of more differentiated tumor cells. Our immunohistochemical analysis of LEKTI expression in matched HNSCC patient specimens confirmed our previous findings of lost or down-regulated LEKTI mRNA transcription in similar specimens (16). We also plan to determine the expression status of severalmMP-9, mMP-14, mMP-3, and KLK5 in HNSCC tumor specimens to expand the relevance of our cell culture-based findings to patient derived tissues.

Conclusion

The enhancement of adhesion to ECM constituents along with the alteration in expression pattern of mMPs in LEKTI expressing clones of OSC19 demonstrates a mechanism of impaired invasive capacity. Our findings define a novel role in which LEKTI provides a critical cellular switch from stationary to migratory cell phases.

Acknowledgements

Supported in part by the NIH-NCI P50 CA097007, NIH R01 DE013954, NIH P30 CA016672, Alando J Ballantyne Distinguished Chair in Head and Neck Surgery award, Michael A. O'Bannon Endowment for Cancer Research, NIH INRS Award T32 CA060374, and AAO-HNSF Percy Memorial Grant.

Conflict of interest

The author declares no conflict of interest.

References

1. Magert HJ, Standker L, Kreutzmann P, et al. LEKTI, a novel 15–domain type of human serine proteinase inhibitor. *J Biol Chem*. 1999;274(31):21499–214502.
2. Chavanas S, Bodemer C, Rochat A, et al. Mutations in SPINK5, encoding a serine protease inhibitor, cause Netherton syndrome. *Nat Genet*. 2000;25(2):141–142.
3. Muller FB, Hausser I, Berg D, et al. Genetic analysis of a severe case of Netherton syndrome and application for prenatal testing. *Br J Dermatol*. 2002;146(3):495–499.
4. Bitoun E, Bodemer C, Amiel J, et al. Prenatal diagnosis of a lethal form of Netherton syndrome by SPINK5 mutation analysis. *Prenat Diagn*. 2002;22(2):121–126.
5. Komatsu N, Takata M, Otsuki N, et al. Elevated stratum corneum hydrolytic activity in Netherton syndrome suggests an inhibitory regulation of desquamation by SPINK5–derived peptides. *J Invest Dermatol*. 2002;118(3):436–443.
6. Bitoun E, Chavanas S, Irvine AD, et al. Netherton syndrome: disease expression and spectrum of SPINK5 mutations in 21 families. *J Invest Dermatol*. 2002;118(2):352–361.
7. Stoll C, Alembik Y, Tchomakov D, et al. Severe hypernatremic dehydration in an infant with Netherton syndrome. *Genet Couns*. 2001;12(3):237–243.
8. Sprecher E, Chavanas S, DiGiovanna JJ, et al. The spectrum of pathogenic mutations in SPINK5 in 19 families with Netherton syndrome:implications for mutation detection and first case of prenatal diagnosis. *J Invest Dermatol*. 2001;117(2):179–187.
9. Descargues P, Deraison C, Bonnart C, et al. Spink5–deficient mice mimic Netherton syndrome through degradation of desmoglein 1 by epidermal protease hyperactivity. *Nat Genet*. 2005;37(1):56–65.
10. Komatsu N, Saijoh K, Jayakumar A, et al. Correlation between SPINK5 gene mutations and clinical manifestations in Netherton syndrome patients. *J Invest Dermatol*. 2008;128(5):1148–1159.
11. Di WL, Hennekam RC, Callard RE, et al. A heterozygous null mutation combined with the G1258A polymorphism of SPINK5 causes impaired LEKTI function and abnormal expression of skin barrier proteins. *Br J Dermatol*. 2009;161(2):404–412.
12. Diociaiuti A, Castiglia D, Fortugno P, et al. Lethal Netherton syndrome due to homozygous p.Arg371X mutation in SPINK5. *Pediatr Dermatol*. 2013;30(4):e65–e67.

13. D'Alessio M, Fortugno P, Zambruno G, et al. Netherton syndrome and its multifaceted defective protein LEKTI. *G Ital Dermatol Venereol*. 2013;148(1):37–51.

14. Walden M, Kreutzmann P, Drogemuller K, et al. Biochemical features, molecular biology and clinical relevance of the human 15–domain serine proteinase inhibitor LEKTI. *Biol Chem*. 2002;383(7–8):1139–1141.

15. Lauber T, Schulz A, Schweimer K, et al. Homologous proteins with different folds:the three–dimensional structures of domains 1 and 6 of the multiple Kazal–type inhibitor LEKTI. *J Mol Biol*. 2003;328(1):205–219.

16. Gonzalez HE, Gujrati M, Frederick M, et al. Identification of 9 genes differentially expressed in head and neck squamous cell carcinoma. *Arch Otolaryngol Head Neck Surg*. 2003;129(7):754–759.

17. Shah TM, Patel AK, Bhatt VD, et al. The landscape of alternative splicing in buccal mucosa squamous cell carcinoma. *Oral Oncol*. 2013;49(6):604–610.

18. Mitsudo K, Jayakumar A, Henderson Y, et al. Inhibition of serine proteinases plasmin, trypsin, subtilisin A, cathepsin G, and elastase by LEKTI: a kinetic analysis. *Biochemistry*. 2003;42(13):3874–3881.

19. Jayakumar A, Kang Y, Mitsudo K, et al. Expression of LEKTI domains 6–9' in the baculovirus expression system:recombinant LEKTI domains 6–9' inhibit trypsin and subtilisin A. *Protein Expr & Purif*. 2004;35(1):93–101.

20. Raghunath M, Tontsidou L, Oji V, et al. SPINK5 and Netherton syndrome: novel mutations, demonstration of missing LEKTI, and differential expression of transglutaminases. *J Invest Dermatol*. 2004;123(3):474–483.

21. Jayakumar A, Kang Y, Henderson Y, et al. Consequences of C–terminal domains and N–terminal signal peptide deletions on LEKTI secretion, stability, and subcellular distribution. *Arch Biochem Biophys*. 2005;435(1):89–102.

22. Schechter NM, Choi EJ, Wang ZM, et al. Inhibition of human kallikreins 5 and 7 by the serine protease inhibitor lympho–epithelial Kazal–type inhibitor (LEKTI). *Biol Chem*. 2005;386(11):1173–1184.

23. Deraison C, Bonnart C, Lopez F, et al. LEKTI fragments specifically inhibit KLK5, KLK7, and KLK14 and control desquamation through a pH–dependent interaction. *Mol Biol Cell*. 2007;18(9):3607–3619.

24. Borgono CA, Michael IP, Komatsu N, et al. A potential role for multiple tissue kallikrein serine proteases in epidermal desquamation. *J Biol Chem*. 2007;282(6):3640–3652.

25. Hachem JP, Wagberg F, Schmuth M, et al. Serine protease activity and residual LEKTI expression determine phenotype in Netherton syndrome. *J Invest Dermatol*. 2006;126(7):1609–1621.

26. Bennett K, Callard R, Heywood W, et al. New role for LEKTI in skin barrier formation: label–free quantitative proteomic identification of caspase 14 as a novel target for the protease inhibitor LEKTI. *J Proteome Res*. 2010;9(8):4289–4294.

27. Jayakumar A, Huang WY, Raetz B, et al. Cloning and expression of the multifunctional human fatty acid synthase and its subdomains in Escherichia coli. *Proc Natl Acad Sci U S A*. 1996;93(25):14509–14514.

28. Henderson YC, Frederick MJ, Jayakumar A, et al. Human LBP–32/MGR is a repressor of the P450scc in human choriocarcinoma cell line JEG–3. *Placenta*. 2007;28(2–3):152–160.

29. Klopp AH, Jhingran A, Ramdas L, et al. Gene expression changes in cervical squamous cell carcinoma after initiation of chemoradiation and correlation with clinical outcome. *Int J Radiat Oncol Biol Phys*. 2008;71(1):226–236.

30. Bitoun E, Micheloni A, Lamant L, et al. LEKTI proteolytic processing in human primary keratinocytes, tissue distribution and defective expression in Netherton syndrome. *Hum Mol Genet*. 2003;12(19):2417–2430.

31. Jayakumar A, Cataltepe S, Kang Y, et al. Production of serpins using baculovirus expression systems. *Methods*. 2004;32:177–184.

32. Roomi MW, Kalinovsky T, Rath M, et al. Modulation of u–PA, MMPs and their inhibitors by a novel nutrient mixture in human female cancer cell lines. *Oncol Rep*. 2012;28(3):768–776.

33. Woessner JF Jr. MMPs and TIMPs—an historical perspective. *Mol Biotechnol*. 2002;22(1):33–49.

Citation: Jayakumar A, Chattopadhyay C, Wu HK, et al. LEKTI, a physiological inhibitor of multiple serine proteinases, blocks migration and invasion of head and neck squamous cell carcinoma (HNSCC) cells. *MOJ Proteomics Bioinform.* 2014;1(3):57–71. DOI: 10.15406/mojpb.2014.01.00015